ORIGINAL ARTICLE

Effect of High-Porosity Endovascular Coiling on Hemodynamics and Thrombosis Formation in Middle Cerebral Artery Aneurysm: A CFD–PIV Study

Aisya Nursaffiya Bt Shaharul Sadri[1], Nadia Shaira binti Shafii[5], Ryuhei Yamaguchi[2], Kahar Osman[3], Mohamad Ikhwan Kori[5], Mohd Rashdan bin Saad[4], Makoto Ohta[2]

[1] Centre of Biomedical Engineering, University of Cyberjaya, Persiaran Cyber 11, 63000 Sepang, Selangor.
[2] Institute of Fluid Science, Tohoku University, 2-1-1 Katahira, 980-8577 Miyagi, Japan.
[3] Faculty of Mechanical Engineering, Universiti Teknologi Malaysia, 81310 UTM Johor Bahru, Johor, Malaysia.
[4] Department of Aeronautics Engineering and Aviation, Faculty of Engineering, Universiti Pertahanan Malaysia, Kem Sungai Besi, 57000 Kuala Lumpur, Malaysia.
[5] Department of Biomedical Engineering and Health Sciences, Faculty of Electrical Engineering, Universiti Teknologi Malaysia, 81310 UTM Johor Bahru, Johor, Malaysia.

ABSTRACT

Introduction: Intracranial aneurysm rupture is one of the asymptomatic diseases that could cause internal bleeding in the brain with high potential for fatality. One of the treatments for aneurysms is an endovascular coil. However, the common related issues to this treatment are recanalization and coil migration. **Materials and Methods:** This study aims to predict the flow behavior and thrombus development through Computational Fluid Dynamics (CFD) simulation by comparing untreated and 0.7 coiled Middle Cerebral Aneurysm (MCA) aneurysm models. In essence, the significance of this study lies in its ability to link coil porosity to thrombus initiation by quantitatively analyzing key hemodynamic parameters. This includes velocity distribution, Wall Shear Stress (WSS), and Pressure Difference (PD) to provide new insights into how coiling can stabilize the aneurysm. **Result:** An experiment was conducted with a only 10.3% difference in velocity. The analyzed hemodynamic parameters that are accountable for the initiation of thrombosis demonstrated that the coiled MCA aneurysm results in a uniform outflow velocity. Specifically, it yields a 17.4% larger area of low WSS (WSS_{low}) and a 35.68% lower PD compared to the untreated MCA aneurysm. **Conclusion:** Overall, these results revealed that high porosity coiling may reduce the risk of migration, rebleeding, and recurrence problems after surgery.
Malaysian Journal of Medicine and Health Sciences (2025) 21(6):1-8. doi:10.47836/mjmhs.v21.i6.1416

Keywords: Computational fluid dynamics, MCA aneurysm, Particle Image Velocimetry (PIV), Coiling, Porosity

Corresponding Author:
Nadia Shaira Shafii, PhD
Email: nadiashaira@utm.my
Tel: +6019-7727572

INTRODUCTION

The intracranial aneurysm formation was caused by the weakening of the artery wall, which can lead to rupture. This aneurysm is an arterial wall dilatation and usually occurs near the arterial bifurcations in the “Circle of Willis” (1). Fig. 1 (a) displays a ruptured blood vessel in the brain that will block the blood, oxygen, and nutrients supply to the brain and lead to a stroke. At the same time, it can lead to Subarachnoid Hemorrhage (SAH), rupture, and death (2). Notably, there are a few types of aneurysms in the Circle of Willis, and the most common type of aneurysm that develops at the blood vessel is a saccular aneurysm (3). Furthermore, to prevent or delay the rupture, one of the common treatments performed to impede blood flow and promote thrombus formation is endovascular coiling (4). In line with this, previous studies reported that the patients who underwent endovascular coiling experienced better outcomes throughout their few years of follow-ups, with a high rate of success and associated with low morbidity (5).

Fig. 1 (b) illustrates the endovascular coil in the saccular aneurysm (6).

(a) (b)

Fig. 1 (a) The ruptured aneurysm that can lead to adverse effects, including Subarachnoid Hemorrhage (SAH); (b) Image of an aneurysm being treated by endovascular (6)

Nonetheless, there are still approximately 40% of procedure-related complications on coil migration that cause the rebleeding and reoccurrence of the aneurysm and lead to a higher risk of rupture (7). The reason for this phenomenon is due to a few factors, including the flow recirculation, permeability, and porosity of the coil. In addition, the blood recirculation inside the aneurysm dome will continue and weaken the aneurysm wall, making it more prone to rupture (8). The flow inside the dome is inconsistent as the formation of vortices and flow recirculation are observed based on the velocity distribution, oscillatory, and WSS (9–12). Moreover, the high porosity coil is crucial as it disrupts the flow entering the area of the aneurysm properly and promotes thrombus formation to help harden the weakened wall, hold the coil, and stop the blood from entering the aneurysm area (13).

Recent studies have emphasized the significance of coil porosity and packing density in modulating intra-aneurysmal hemodynamics. As studied by (14), the hemodynamic consequences of different coil porosities were noted using Computational Fluid Dynamics (CFD) simulations. The study also reported that reduced porosity substantially damps inflow velocity and minimizes oscillatory shear, creating a more thrombogenic environment conducive to aneurysm occlusion. Complementarily, (15) extended this work by comparing untreated and coiled aneurysm models across multiple packing densities. The authors demonstrated that higher packing densities lead to lower intra-aneurysmal pressure gradients and larger regions of low Wall Shear Stress (WSS), both of which are predictive of stable thrombus formation and reduced risk of recurrence. Together, these studies provide strong evidence that optimizing coil porosity is crucial for achieving favorable post-treatment hemodynamics. Additionally, it directly motivates the present study's quantitative analysis of a 0.7 porosity coiled MCA aneurysm model using velocity, WSS, and Pressure Difference (PD) as predictive indicators for thrombus development.

Therefore, this study aims to predict the flow behavior and thrombus development through computational simulation by comparing the untreated and 0.7 coiled MCA aneurysm models. Since thrombosis formation is essential for securing the coil and maintaining aneurysm occlusion, the hemodynamic analysis focuses on velocity distribution, WSS, and PD. This seeks to evaluate the potential of high-porosity coiling in reducing the risks of coil migration, rebleeding, and recurrence.

MATERIALS AND METHODS

Modeling and numerical simulation

The simplified models of MCA with aneurysm model were constructed based on the parameters that were referred to the patient-specific image (16,17) using the Computational Aided Software (CAD), SOLIDWORKS (Dassault Systиmes SolidWorks Corporation, Waltham, MA). Meanwhile, the porosity of the attached coil model (70% porosity or 0.7), as displayed in Fig. 2 (b), was determined using a formula Porosity (ш) = (Total volume/Volume void) (18). Accordingly, the coil volume was estimated based on the aneurysm sac volume and the desired packing density, and the porous domain was assigned an equivalent flow resistance following Darcy's law approach to represent the hemodynamic impact of the coil mass. This approach is consistent with previous studies (19) that validated the porous medium method for simulating endovascular coiling in patient-specific aneurysm geometries. Moreover, coil porosity is the fraction of the aneurysm volume that remains unfilled by the deployed coils. However, it is not the same as material porosity, which refers to microscopic voids within the coil material itself (20). Following this, the generated meshing and boundary conditions are simulated in ANSYS CFD Fluent (Canonsburg, PA, USA). The constructed models employed in simulation and experiment were scaled 1:2 to the actual geometry, as the full-scale geometry is overly complex for the early flow visualization process.

(a) (b)

Fig. 2 (a) Untreated MCA aneurysm simplified model; (b) The 0.7 coiled MCA aneurysm

A steady state inlet velocity of 1.3 m/s was imposed at the inlet based on earlier research (21). The laminar flow model was selected due to its low Reynolds number and non-slip boundary condition, with the focus of this paper being mainly on the flow properties away from the wall. Both outlet vessels' flow rates were kept constant at the same free flow rate. Additionally, the blood used in this simulation was treated as an incompressible Newtonian fluid with a viscosity of 0.0035 N. s/m2 and a density of 1,060 kg/m^3. For the entire flow domain, a triangular mesh (tetrahedral) was chosen since mesh quality significantly impacts the accuracy of the numerical solutions. Specifically, there were 4,727,971 elements and 1,018,752 nodes in the meshing configuration.

Hemodynamic Parameters

There are a few parameters that relate to the thrombosis formation, such as velocity vortex distribution, PD, WSS, and percentage area of WSS_{low} (22,23). The velocity vortex distribution is vital to monitor the flow recirculation and vortex formation that could cause the coil migration. It also impacts the distribution of oxygen and nutrients through the blood flow, as the brain's function is to carry oxygen-rich blood to the body parts (24–26). The next parameter to be considered in this study is a PD, which is essential in helping define the degree of pressure elevation for the neck plane. Note that a higher PD value will promote the recanalization problem after the coiling treatment (27) The PD equation (1) is given below, where P_{max} was calculated as the highest value of pressure in the neck planes. Meanwhile, P_{ave} was calculated as the mean value of the pressure at the inlet plane. Moreover, V_{in} was calculated as the average flow velocity at the inlet plane in meters per second, and ρ is the density.

$$PD = \frac{P_{max} - P_{ave}}{\frac{1}{2}\rho v_{in}^2} \quad (1)$$

The evaluation for WSS, τ, and its maximum referred to equation (2), where μ is the blood dynamic viscosity and r is the radial direction perpendicular to the arterial wall. WSS is one of the crucial parameters, and in complex patient-specific body models, the complexity leads to irregularity of blood flow. Meng et al, (28) discussed that high WSS contributes to aneurysm formation. Correspondingly, a high WSS (more than 3.0 Pa) induces high jetting flow inside the healthy brain vessel and can promote blood clots or stroke (Leonid Goubergrits et al., 2011; Sotelo et al., 2016). It will also decrease the stiffness of the brain vessel (Safar et al., 2018). In addition, coil embolization addresses intrasaccular blood thrombosis by inducing clot formation within the aneurysm sac, isolating the aneurysm from the systemic circulation. Essentially, a low WSS (WSS_{low}) (0-1.5 Pa) promotes effective thrombosis (29). Thus, areas with WSS_{low} will also be observed to evaluate the blood absorption efficiency before and after coiling treatment in this study.

$$\tau = \mu \frac{dU}{dr} \quad (2)$$

Particle Image Velocimetry Experiment Validation
The experiment was conducted by applying the Particle Image Velocimetry (PIV) technique before the simulation. The velocities were measured by a two-dimensional method with light intensity for both frames. The laser label is 11 with dt = 807.49 microseconds, while the PIV captured 100 images in 7.73 seconds. The measurement was performed at the median xy plane with a Reynolds number = 310 and water as the flow medium. Subsequently, a coiled MCA aneurysm with high porosity was fabricated. The validation was measured based on the velocity line on the median plane for simulation and experiment. Fig. 3 illustrates the schematic diagram and full setup of the experiment. The PIV system comprises the CCD Imager SX6M camera, which has a resolution of 2,752 x 2,200 pixels, with high-power supplied by Teledyne Imaging. It also features a double-pulsed Quantel Evergreen 200 Nd laser, manufactured by the EverGreen Hp, a flexible laser guiding arm, and adjustable optics with interchangeable lenses (30).

RESULT

This study was started by modeling and fabrication for conducting the flow visualization and validation experiment using PIV. This is followed by a simulation using the ANSYS CFD Fluent (Canonsburg, PA, USA) to analyze hemodynamic parameters and study the thrombosis formation in holding the coil for MCA aneurysm between the untreated MCA aneurysm (UT) and the coiled MCA aneurysm. The relationship between velocity vortex distribution, PD, and WSS with the maximum value is analyzed, as displayed in Fig. 3

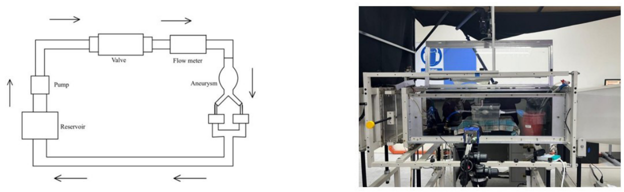

(a) (b)

Fig. 3 (a) The experiment schematic diagram; (b) The PIV setup

Particle Image Velocimetry Experiment (PIV) and CFD Validation
The PIV approach was employed to validate the numerical results both qualitatively and quantitatively. The validation focused on the velocity distribution within the coiled MCA aneurysm model, where the velocity field and its profile were compared between the PIV experiment and CFD simulation.

Fig. 4 illustrates the median plane selected for analysis; Fig. 4 (a) represents the PIV experimental result, while Fig. 4 (b) depicts the CFD prediction at the same Reynolds number. The plane passes through both the inlet and outlet, allowing an effective comparison of flow patterns. As the flow enters the aneurysm dome, a reduction in velocity magnitude is observed due to the larger cross-sectional area relative to the inlet artery, which is consistent with the principle of conservation of mass. At the same time, the CFD result reveals similar flow behavior, with good qualitative agreement in the velocity field and recirculation regions.

To provide a more quantitative comparison, the velocity profile was extracted along the line indicated in Fig. 5 (a) and plotted for both methods in Fig. 5 (b). The comparison suggests that the CFD simulation captures the overall velocity trend observed in the PIV data, with close agreement at peak velocity locations. In addition, the trend demonstrates good agreement between the CFD and PIV results, and the slight deviation may be due to differences in the material used in the experiment. This is as agreed with the findings reported in other PIV-CFD validation studies (15,31).

The experimental setup involved seeding density control, accurate calibration, and precise laser sheet alignment, in line with recommended best practices for experimental validation of computational hemodynamics, as conducted by these studies (32,33). These steps ensured higher accuracy, improving the reliability of the comparison between experimental and numerical results.

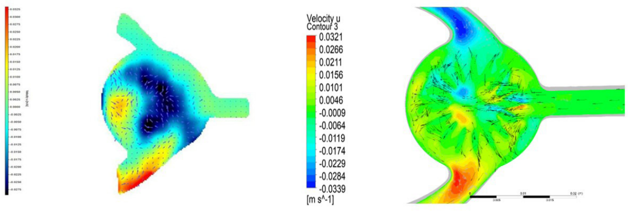

(a) (b)

Fig. 4 Flow behavior on the median plane for (a) Untreated MCA aneurysm (UT); (b) 0.7 coiled aneurysm

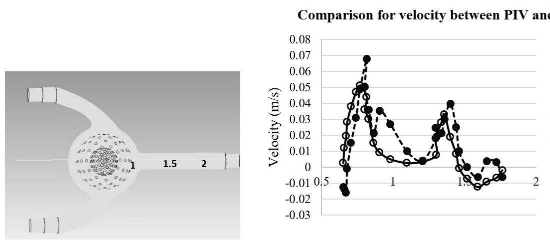

(a) (b)

Fig. 5 (a) The line on the median plane; (b) The velocity comparison between CFD and PIV

Velocity vortex distribution

Fig. 6 displays the flow velocity vortex distribution compared between the untreated MCA aneurysm and the 0.7 coiled MCA aneurysm. The flow in the aneurysm starts by entering the neck and swirling to the left area of the dome. These observed vortex- and velocity distribution patterns in our 0.7 coiled MCA model are consistent with recent findings by (21,34). The study reported increased flow eddies, flow stagnation, and positive WSS divergence in thrombosed intracranial aneurysms compared to non-thrombosed ones. Meanwhile, (35) identified high residence time and low shear rate as key triggers for spontaneous thrombosis initiation in large and giant aneurysm phenotype.

Wall shear stress (WSS) and Percentage area of WSS_{low}

WSS is the viscous drag exerted by flowing blood on the arterial wall, as presented in Fig. 6 (c) and (d). In particular, the blue color indicates the low magnitude of WSS or WSS_{low}. WSS_{low} with less than 3.0 Pa was discussed seriously in recent studies (36) as it is related to the formation of thrombosis. These WSS_{low} areas indicate disturbed flow and reduced tangential forces on the vessel wall, conditions that are well known to predispose to thrombus initiation and vascular remodeling. Furthermore, the result reveals that a larger area of WSS_{low} (< 3.0 Pa) in Fig. 6 (d) compared to Fig. 6 (c), with these regions overlapping the disturbed velocity fields, as observed in Fig. 6 (a) and (b). These extended WSS_{low} areas are crucial since they represent areas where the vessel wall is more vulnerable to thrombus formation and plaque development. Additionally, this finding is clinically relevant, as larger regions of WSS_{low} strongly contribute to thrombus formation and plaque progression, aligned with observations in clinical studies by Hartman et al. (37)

WSS is the viscous drag exerted by flowing blood on the arterial wall, as illustrated in Fig. 6 (c) and (d). The blue regions indicate WSS_{low}, typically defined as less than 3.0 Pa, which has been highlighted in recent studies (36) as a critical factor associated with thrombus formation. As such, these WSS_{low} areas reflect disturbed flow and reduced tangential forces on the vessel wall, conditions known to predispose to thrombus initiation and vascular remodeling. The results reveal a larger area of WSS_{low} in Fig. 7 (a), with these regions overlapping the disturbed velocity fields observed in Fig. 6 (a) and (b). Notably, coil porosity has a direct influence on these hemodynamic patterns. Previous studies suggest that a porosity of approximately 0.7 provides an optimal balance by sufficiently reducing intra-aneurysmal inflow to expand regions of WSS_{low}, while still allowing gradual thrombus organization (28). Clinically, this finding is highly relevant, since larger regions of WSS_{low} have been strongly associated with thrombus formation and plaque progression, consistent with observations by Hartman et al. (37).

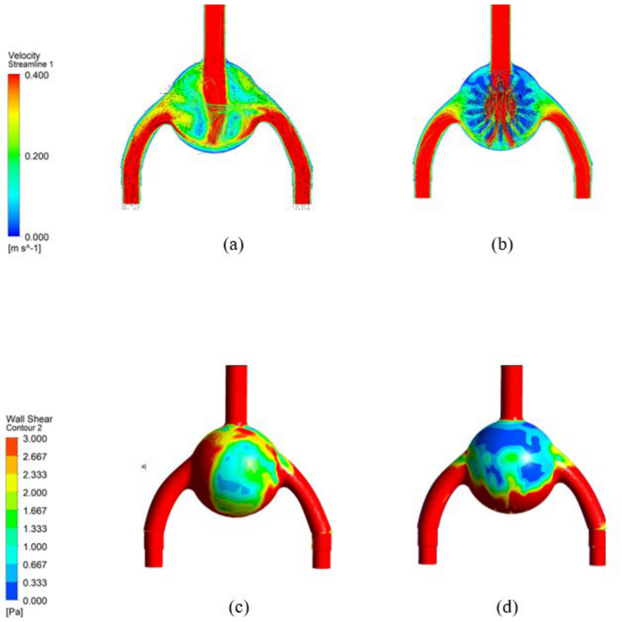

Fig. 6 The flow velocity streamline for (a) an Untreated MCA aneurysm (UT); and (b) a 0.7 coiled MCA aneurysm. The contour plot for wall shear stress (WSS) for (c) Untreated MCA aneurysm (UT); and (d) 0.7 MCA aneurysm

Pressure Difference, PD

Fig. 7 (b) illustrates that the 0.7 coiled MCA aneurysm PD is lower than that of the untreated MCA aneurysm, indicating the recurrence risk of happening in the coiled MCA aneurysm is 35.68% lower. Therefore, this reflects the hemodynamic stabilizing effect of reduced pressure gradients, which is supported by other computational studies indicating that coiling decreases the range of intra-aneurysmal pressures by dampening pressure peaks and elevating troughs, attenuating PDs within the sac (38).

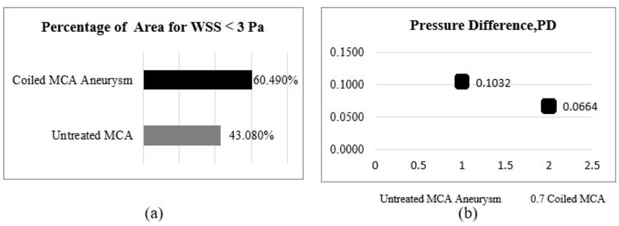

Fig. 7 (a) The area of the aneurysm dome with WSS_{low}; (b) The PD between the UT MCA aneurysm and the 0.7 coiled MCA aneurysm

DISCUSSION

Based on the validation results in Figs. 4 and 5, both contours resulted in almost a similar pattern once the flow enters where vortices form at the centre to the end side of the aneurysm dome. The gravity effect setting was applied, and the result of the outflow demonstrates higher values at the bottom side outlet and slower at the top area. Meanwhile, the flow behavior is lower at the center of the aneurysm dome due to the coil presence inside the aneurysm dome, as demonstrated in the previous study regarding the flow distribution. To quantify this, as the flows pass through the aneurysm, Fig. 5 (b) illustrates the comparison of the velocity values with good agreement and only a 10.3% difference. Note that both results use the same legend scales and identical maximum values.

For the velocity vortex distribution, high jetting flow impact at the end of the aneurysm wall can be observed in an untreated MCA aneurysm. This could weaken the wall and lead to rupture. Hence, observing the flow distribution in the untreated aneurysm (a) revealed clear vortex formation due to the flow disturbance, which led to unbalanced outflow distribution to both outlets. Consistent with this, many adverse effects could be caused by the flow disturbance and unbalanced outflow, such as oxygen and nutrient insufficiency in other body parts. For the coiled aneurysm, the flow velocity in Fig.6 (b) is low at the center of the aneurysm dome, which helps uniform outflow behavior on both outlets. Furthermore, a large area was observed with a low-velocity vortex distribution, potentially leading to a stagnation point at the center. This condition is expected to accelerate thrombosis formation, preventing coil migration out of the aneurysm dome in the 0.7 coiled MCA aneurysm compared to the untreated model.

One of the critical parameters to be analyzed is WSS. The result, as presented in Fig. 6 (c) and (d), indicates a larger area with WSS_{low} in the 0.7 coiled MCA aneurysm, with 60.49% area recorded and for the untreated MCA aneurysm, only with 43.08% area of WSS_{low}. The value is presented in Fig. 7 (a). This phenomenon revealed that the shear stress on the aneurysm wall is reduced once the 0.7 coiled MCA aneurysm is used to treat the aneurysm, which then expedites the thrombus formation to close the aneurysm sac (39,40).

One of the other relevant parameters to be analyzed in predicting the recurrence after coiling treatment is PD, as displayed in Fig. 7. A higher PD value will promote the recanalization problem after the coiling treatment (41). High-PD conditions will allow more flow to enter the aneurysm sac, which then exhibits irregular behavior as discussed in the previous study (41). Overall, in this study, a reduction in intra-aneurysmal velocity, an enlargement of WSS_{low} regions, and a more uniform flow distribution were observed in the 0.7 coiled MCA aneurysm. These findings align with those reported by Morales et al. (42), who demonstrated that coiling at a packing density of approximately 30% can significantly lower intra-aneurysmal velocity and WSS while preserving the overall flow pattern. Accordingly, this agreement strengthens confidence in the computational approach used here. It also highlights the potential of porosity-based coil modeling as a tool for predicting hemodynamic conditions that encourage thrombus formation and improve coil stability.

CONCLUSION

The formation and growth of thrombosis are key to preventing coil migration and recurrence after endovascular coiling treatment. In this work, we analyzed hemodynamic parameters, including velocity vortex distribution, WSS, percentage area of $WSS_{low,}$ and PD. The result revealed that the 0.7 coiled MCA aneurysm created more favorable flow conditions, encouraging thrombus formation and improving coil stability. These observations are in line with the findings of Morales et al. (2013), who also reported reductions in intra-aneurysmal velocity and WSS following coil embolization. Taken together, these results indicate that optimizing coil porosity may help lower the risks of coil migration, rebleeding, and recurrence, providing a strong basis for future work exploring the relationship between porosity and thrombosis.

ACKNOWLEDGEMENTS

This project was supported by an International Joint Grant with the Institute of Fluid Science (IFS), Tohoku University, Japan, (project code no: J24I087, J51017) and the Collaborative Research and External Grant with code No: 4Y350, 4Y375, Universiti Teknologi Malaysia. Also, the experimental support from the team of the Department of Aeronautics Engineering and Aviation, Faculty of Engineering, National Defence University Malaysia is gratefully acknowledged. This research does not include any experiments or data involving human participants or animal subjects, and therefore, ethical approval is not required.

REFERENCE

1. Keedy A. An overview of intracranial aneurysms. McGill Journal of Medicine. 2006;9(2):141-146. doi: 10.26443/mjm.v9i2.672
2. Kojima M, Tercero CR. The effect of Mesh Design in Cerebral Aneurysm Hemodynamics for Developing Flow Controllable Stent : Computational Fluid Dynamics Study. Published online 2012:772-777. doi:10.1109/ICCME.2012.6275740
3. Juvela S. Prehemorrhage risk factors for fatal intracranial aneurysm rupture. Stroke. 2003;34(8):1852-1857. doi:10.1161/01.STR.0000080380.56799.DD
4. Tominari S, Morita A, Ishibashi T, et al. Prediction model for 3-year rupture risk of unruptured cerebral aneurysms in Japanese patients. Ann Neurol. 2015;77(6):1050-1059. doi:10.1002/ana.24400
5. Zhang M, Li Y, Zhao X, et al. Haemodynamic effects of stent diameter and compaction ratio on flow-diversion treatment of intracranial aneurysms: A numerical study of a successful and an unsuccessful case. J Biomech. 2017;58:179-186. doi:10.1016/j.jbiomech.2017.05.001
6. Mascitelli J, Howington JU. Anterior communicating artery aneurysms. In: Intracranial Aneurysms. Elsevier; 2018:463-478. doi:10.1016/B978-0-12-811740-8.00029-0
7. Sellar R. Complications of interventional treatment of cerebral aneurysms. Interventional Neuroradiology. 2008;14(SUPPL. 1):63-74. doi:10.1177/15910199080140s112
8. Shafii NS, Yamaguchi R, Tanaka G, et al. PATIENT SPECIFIC IMAGES IN THE MIDDLE CEREBRAL ARTERY ANEURYSM SIMULATION WITH TURBULENT MODEL. 2019;(June):635-638.
9. Baek H, Jayaraman M V., Richardson PD, Karniadakis GE. Flow instability and wall shear stress variation in intracranial aneurysms. J R Soc Interface. 2010;7(47):967-988. doi:10.1098/rsif.2009.0476
10. Hajirayat K, Gholampour S, Seddighi AS, Fatouraee N. Evaluation of Blood Hemodynamics in Patients with Cerebral Aneurysm. 2016;3(1):44-50.doi: 10.22037/icnj.v3i1.12460
11. Shafii NS, Yamaguchi R, Khudzari AZM, et al. Hemodynamic and Flow Recirculation Effect on Rupture Prediction of Middle Cerebral Artery Aneurysm. Journal of Advanced Research in Fluid Mechanics and Thermal Sciences. 2020;79(1):1-16. doi:10.37934/arfmts.79.1.116
12. Valencia A, Solis F. Blood flow dynamics and arterial wall interaction in a saccular aneurysm model of the basilar artery. Comput Struct. 2006;84(21):1326-1337. doi:10.1016/j.compstruc.2006.03.008
13. Taib I, Amirnordin H, Madon H. The Effect of Flow Recirculation on Abdominal Aortic Aneurysm. 2012;135(Imat 2011):130-135. doi:10.1063/1.4704211
14. Mirzaei Poueinak M, Abdollahi SA, Alizadeh A, Youshanlui MA, Zekri H, Gerdroodbary MB. Computational study of blood hemodynamic in ICA aneurysm with coiling embolism. International Journal of Modern Physics C. 2023;34(10). doi:10.1142/S0129183123501383
15. Dian W, Zhang W, Fu S, et al. Evaluation of coiling endovascular technique on treatment of middle cerebral artery cerebral aneurysms in different blood hematocrits: A numerical study. International Journal of Modern Physics C. 2025;36(07). doi:10.1142/S0129183124502528
16. Yamaguchi R, Kotani T, Tanaka G, et al. Effects of Elasticity on Wall Shear Stress in Patient-Specific Aneurysm of Cerebral Artery. Published online 2019:73-86. doi:10.4236/jfcmv.2019.72006
17. Shafii NS, Yamaguchi R, Khudzari AZM, et al. Hemodynamic and Flow Recirculation Effect on Rupture Prediction of Middle Cerebral Artery Aneurysm. Journal of Advanced Research in Fluid Mechanics and Thermal Sciences. 2020;79(1). doi:10.37934/arfmts.79.1.116
18. Flint LE, Flint AL. Porosity. In: Methods of Soil Analysis, Part 4: Physical Methods. wiley;

2018:241-254. doi:10.2136/sssabookser5.4.c11
19. Wang Y, Jin J, Chen J, Chen P, Abdollahi SA. Impacts of morphology parameters on the risk of rupture in intracranial aneurysms: statistical and computational analyses. Sci Rep. 2023;13(1). doi:10.1038/s41598-023-46211-y
20. Romero Bhathal J, Marsh L, Levitt MR, Geindreau C, Aliseda A. Towards Prediction of Blood Flow in Coiled Aneurysms Before Treatment: A Porous Media Approach. Ann Biomed Eng. 2023;51(12):2785-2801. doi:10.1007/s10439-023-03340-9
21. Shafii NS, Yamaguchi R, Khudzari AZM, et al. Hemodynamic and Flow Recirculation Effect on Rupture Prediction of Middle Cerebral Artery Aneurysm. Journal of Advanced Research in Fluid Mechanics and Thermal Sciences. 2020;79(1):1-16. doi:10.37934/arfmts.79.1.116
22. Taib I, Tun U, Onn H, et al. An analysis of blood pressure waveform using windkessel model for normotensive and hypertensive conditions in carotid artery Journal of Advanced Research in Fluid An Analysis of Blood Pressure Waveform using Windkessel Model for Normotensive and Hypertens. 2019;(May).
23. Darlis N, Osman K, Padzillah MH, Dillon J, Md Khudzari AZ. Modification of Aortic Cannula With an Inlet Chamber to Induce Spiral Flow and Improve Outlet Flow. Artif Organs. 2018;42(5):493-499. doi:10.1111/aor.13021
24. Starke R, Chalouhi N, Ali M, et al. The Role of Oxidative Stress in Cerebral Aneurysm Formation and Rupture. Curr Neurovasc Res. 2013;10(3):247-2
25. Avrahami I, Dilmoney B, Hirshorn O, Brand M, Cohen O, Shani L, et al. Numerical investigation of a novel aortic cannula aimed at reducing cerebral embolism during cardiovascular bypass surgery. J Biomech. 2013;46(2):354–61.
26. Liu X, Fan Y, Deng X. Effect of spiral flow on the transport of oxygen in the aorta: A numerical study. Ann Biomed Eng. 2010;38(3):917–26.
27. Uno T, Misaki K, Nambu I, Yoshikawa A, Kamide T, Uchiyama N, et al. Prediction of internal carotid artery aneurysm recurrence by pressure difference at the coil mass surface. Neuroradiology. 2021;63(4):593–602.
28. Hariri S, Mirzaei Poueinak M, Hassanvand A, Barzegar Gerdroodbary M, Faraji M. Effects of blood hematocrit on performance of endovascular coiling for treatment of middle cerebral artery (MCA) aneurysms: Computational study. Interdiscip Neurosurg. 2023 Jun 1;32.
29. Methal Z, Aat S, Mra R, Mr S. UPNM SUBSONIC WIND TUNNEL FLOW MEASUREMENTS TECHNIQUE AND CALIBRATION.
30. Medero R, Falk K, Rutkowski D, Johnson K, Rold6n-Alzate A. In Vitro Assessment of Flow Variability in an Intracranial Aneurysm Model Using 4D Flow MRI and Tomographic PIV. Ann Biomed Eng. 2020 Oct 10;48(10):2484–93.
31. Yamaguchi R, Albadawi M, Shafii NS, Saito A, Nakata T, Saqr KM, et al. Effects of wall compliance on pulsatile flow in a full-scale, patient-specific cerebral aneurysm model: Particle image velocimetry experiments. Med Eng Phys. 2025 Aug;142:104381.
32. Yamaguchi R, Tanaka G, Shafii NS, Osman K, Shimizu Y, Saqr KM, et al. Characteristic Effect of Wall Elasticity on Flow Instability and Wall Shear Stress of a Full-Scale, Patient-Specific Aneurysm Model in the Middle Cerebral Artery : An Experimental A ... Characteristic Effect of Wall Elasticity on Flow Instability and Wal. 2022;(May).
33. Liu Q, Sarrami-Foroushani A, Wang Y, MacRaild M, Kelly C, Lin F, et al. Hemodynamics of thrombus formation in intracranial aneurysms: An in silico observational study. APL Bioeng. 2023 Sep 1;7(3).
34. Liu Q, Sarrami-Foroushani A, Wang Y, MacRaild M, Kelly C, Lin F, et al. Hemodynamics of thrombus formation in intracranial aneurysms: an in-silico observational study [Internet]. 2022. Available from: https://www.researchsquare.com/article/rs-2371503/v1
35. Dabagh M, Nair P, Gounley J, Frakes D, Fernando Gonzalez L, Randles A. Hemodynamic and morphological characteristics of a growing cerebral aneurysm. Neurosurg Focus. 2019;47(1):1–10.
36. Hartman EMJ, De Nisco G, Gijsen FJH, Korteland SA, van der Steen AFW, Daemen J, et al. The definition of low wall shear stress and its effect on plaque progression estimation in human coronary arteries. Sci Rep. 2021 Dec 1;11(1).
37. Meng H, Tutino VM, Xiang J, Siddiqui A. High WSS or Low WSS? Complex interactions of hemodynamics with intracranial aneurysm initiation, growth, and rupture: Toward a unifying hypothesis. American Journal of Neuroradiology. 2014;35(7):1254–62.
38. Larrabide I, Aguilar ML, Morales HG, Geers AJ, Kulcsar Z, Rufenacht D, et al. Intra-aneurysmal pressure and flow changes induced by flow diverters: Relation to aneurysm size and shape. American Journal of Neuroradiology. 2013 Apr;34(4):816–22.
39. Li Z, Hu L, Chen C, Wang Z, Zhou Z, Chen Y. Hemodynamic Performance of Multilayer Stents in the Treatment of Aneurysms with a Branch Attached. Sci Rep [Internet]. 2019;9(1):1–10. Available from: http://dx.doi.org/10.1038/s41598-019-46714-7
40. Liu X, Wang M, Zhang N, Fan Z, Fan Y, Deng X. Effects of endothelium, stent design and deployment on the nitric oxide transport in stented artery: a potential role in stent restenosis and thrombosis. Med Biol Eng Comput. 2015;53(5):427–39.
41. Nambu I, Misaki K, Uchiyama N, Mohri M, Suzuki T, Takao H, et al. High Pressure in Virtual

Postcoiling Model is a Predictor of Internal Carotid Artery Aneurysm Recurrence after Coiling. Clin Neurosurg. 2019 Mar 1;84(3):607–15.
42. Morales HG, Larrabide I, Geers AJ, Aguilar ML, Frangi AF. Newtonian and non-Newtonian blood flow in coiled cerebral aneurysms. J Biomech. 2013 Sep;46(13):2158–64.